Accepted Manuscript

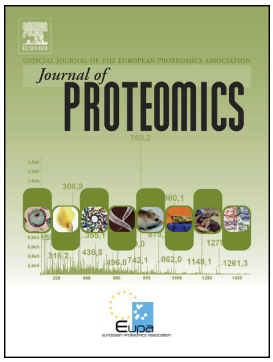

First look into the venom of Roatan Island's critically endangered coral snake Micrurus ruatanus: Proteomic characterization, toxicity, immunorecognition and neutralization by an antivenom

Enikő Lippa, Ferenc Török, Aarón Gómez, Greivin Corrales, Danilo Chacón, Mahmood Sasa, José María Gutiérrez, Bruno Lomonte, Julián Fernández

PII: S1874-3919(19)30015-6
DOI: https://doi.org/10.1016/j.jprot.2019.01.007
Reference: JPROT 3305

To appear in: *Journal of Proteomics*

Received date: 16 December 2018
Revised date: 11 January 2019
Accepted date: 14 January 2019

Please cite this article as: Enikő Lippa, Ferenc Török, Aarón Gómez, Greivin Corrales, Danilo Chacón, Mahmood Sasa, José María Gutiérrez, Bruno Lomonte, Julián Fernández , First look into the venom of Roatan Island's critically endangered coral snake Micrurus ruatanus: Proteomic characterization, toxicity, immunorecognition and neutralization by an antivenom. Jprot (2019), https://doi.org/10.1016/j.jprot.2019.01.007

First look into the venom of Roatan Island´s critically endangered coral snake *Micrurus ruatanus*: Proteomic characterization, toxicity, immunorecognition and neutralization by an antivenom

Enikő Lippa[a], Ferenc Török[b], Aarón Gómez[c], Greivin Corrales[c], Danilo Chacón[c], Mahmood Sasa[c], José María Gutiérrez[c], Bruno Lomonte[c], Julián Fernández[c,*]

julian.fernandezulate@ucr.ac.cr

[a]Department of Human Genetics, University of Debrecen, Debrecen, Hungary

[b]Department of Biophysics and Cell Biology, University of Debrecen, Debrecen, Hungary

[c]Instituto Clodomiro Picado, Facultad de Microbiología, Universidad de Costa Rica, San José, Costa Rica

[*]Corresponding author at: Instituto Clodomiro Picado, Universidad de Costa Rica, San José 11501, Costa Rica.

Abstract

A proteomic and toxicological study of the venom from one specimen of *Micrurus ruatanus,* a critically endangered coral snake species endemic to Roatan Island, Honduras, was carried out. Immunorecognition and neutralization of venom lethality by an anticoral antivenom was also evaluated. Forty peaks were collected from RP-HPLC fractionation of the venom. After SDS-PAGE analysis, fifty-eight bands were examined by MALDI-TOF/TOF mass spectrometry. *Micrurus ruatanus* venom displayed a three-finger toxin (3FTx)-rich venom phenotype, as well as a significant amount of phospholipases A_2 (PLA_2s). Various other proteins were identified, including Kunitz-type inhibitor proteins, L-amino acid oxidases, C-type lectin/lectin-like, metalloproteinases, serine proteinases, vespryn/ohanin, 5'-nucleotidases, glutathione peroxidases, and phosphodiesterases. *Micrurus ruatanus* venom displayed significant PLA_2 activity *in vitro* and myotoxicity *in vivo*. The venom showed high lethal potency in mice, being one of the most lethal in Central America. The anticoral antivenom (SAC-ICP) produced by Instituto Clodomiro Picado neutralized the lethal activity of the venom. Major fractions with relevant lethal activity were also identified by a screening analysis.

Keywords: Venomics, *Micrurus ruatanus*, Coral Snake

Significance

The proteomic characterization, toxicity, immunorecognition and neutralization of *Micrurus ruatanus* venom have been determined for the first time. This coral snake is endemic to Roatan Island and contains a three-finger toxin-rich venom that displayed a potent lethal activity in mice. The anticoral antivenom produced by Instituto Clodomiro Picado neutralized the lethal activity of this venom *in vivo*, and therefore should be effective in the treatment of envenomings by this snake.

1. Introduction

Micrurus ruatanus is a bicolored venomous coral snake species that inhabits the Caribbean island of Roatan in Honduras [1–3]. This species has been categorized as critically endangered by the International Union for Conservation of Nature (IUCN). *Micrurus ruatanus* is the only venomous snake on this island, which has a human population of approximately 45 000 and an estimated area of 83 km^2. Adults of *M. ruatanus* are 50-60 cm long, with a pattern of dark red and black rings (Campbell and Lamar, 2004; Wilson et al., 1992; Fig.1A). *Micrurus ruatanus* is considered a different species from *M. nigrocinctus* since the former has a higher number of black body rings, lower ventral scale number, and a smaller body size than the latter [1].

Bites caused by *M. ruatanus* are rare due to its low abundance, but at least one fatal envenoming has been recorded [3]. Venoms from *Micrurus* species cause neurotoxic alterations such as paresthesia, local pain, ptosis, nausea, diplopia, ophthalmoplegia, and bulbar paralysis associated with dysarthria and dysphagia [5,6]. In severe cases, respiratory paralysis that leads to death has been reported [5].

Virtually no information is known on the venom of *M. ruatanus*, due to the fact that the snake is critically endangered and therefore specimens and venom are extremely hard to obtain. Based on the snake venomics platform [7–9], previous studies of the composition of coral snake venoms have shown that they are mainly composed of three finger toxins

(3FTxs) and phospholipases A_2 (PLA_2s), with a predominant abundance of one of these toxin types, depending on the species [10,11].

We report the proteomic analysis of the venom from a specimen of this species, as well as a characterization of its toxic and PLA_2 activities, the neutralization of lethality, and immunorecognition by an anticoral antivenom produced at Instituto Clodomiro Picado, Costa Rica.

2. Materials and methods

2.1. Snake venom and antivenom

Venom was collected in March, June, and September of 2018 from one *M. ruatanus* female adult specimen, kept at the Serpentarium of Instituto Clodomiro Picado, University of Costa Rica, after it was confiscated in 2006 by Costa Rican authorities. After extraction, the venom samples were lyophilized, pooled, and stored at -20℃ until analysis. Immunoassays and neutralization experiments were performed with the equine antivenom raised against the coral snake *M. nigrocinctus* (SAC-ICP) produced by Instituto Clodomiro Picado, University of Costa Rica (Batch 6040518, protein concentration: 2.64 ± 0.05 g/dL, expiry date: May 2021). Protein quantification was performed by measuring the absorbance at 280 nm and assuming a 1 mg/mL concentration for 1.0 absorbance, using a NanoDrop 2000C instrument (Thermo Scientific, Waltham, Massachusetts, United States).

2.2. RP-HPLC and SDS-PAGE

Venom samples (2.2 mg) were dissolved in 200 µL of solution A (0.1% trifluoroacetic acid; TFA), centrifuged at 15,000 x g for 5 min to remove debris, and separated on a C18 column (250 x 4.6 mm, 5 µm particle size; Teknokroma) using an Agilent 1200 chromatograph with detection at 215 nm. Elution was performed at 1 mL/min by applying the following gradient toward solution B (0.1% TFA in acetonitrile): 0% B for 5 min, 0-15% B over 10 min, 15-45% B over 60 min, 45-70% B over 10 min, and 70% B over 9 min [12]. Fractions were collected manually, dried in a vacuum centrifuge (SpeedVac, Thermo), redissolved in water, and separated by SDS-PAGE in pre-cast 4-20% gels (Sigma–TruPage™) under reducing conditions. After LabSafe GEL Blue™ staining, protein bands were cut from gels and subjected to reduction (10 mM dithiothreitol), alkylation (50 mM iodoacetamide), and overnight in-gel digestion with sequencing grade bovine trypsin (in 25 mM ammonium bicarbonate) using an automated digestor (DigestPro MSi, Intavis, Cologne, Germany). The peptides were extracted with 0.1% TFA in 60% acetonitrile and concentrated for tandem mass spectrometry.

2.3. MALDI-TOF/TOF

Tryptic peptides were mixed with an equal volume of saturated α-cyano-4-hydroxycinnamic acid matrix (in 50% acetonitrile, 0.1% TFA), spotted (1.5 µL) onto Opti-TOF 384 plates, dried, and analyzed in positive reflector mode using a Proteomics Analyzer 4800-Plus instrument (Sciex, Washington D.C., USA). Spectra were acquired using a laser intensity of 3000 and 500 shots/spectrum, using as external standards CalMix-5 (Sciex) spotted on the same plate. Up to 10 precursor peaks from each MS spectrum were

selected for automated collision-induced dissociation MS/MS spectra acquisition at 2 kV, in positive mode (500 shots/spectrum, laser intensity 3500). Resulting spectra were searched using the Paragon® algorithm of ProteinPilot v.4 (Sciex) against the UniProt/SwissProt database for Serpentes, at a confidence level of ≥95%, for the assignment of proteins to known families. A few peptides with lower confidence scores were manually searched using BLAST (http://blast.ncbi.nlm.nih.gov), and their sequence was confirmed manually.

2.4. Protein family composition of venom

The relative abundance of each protein (% of total venom proteins) was estimated by integration of the RP-HPLC peak signals at 215 nm, using Chem Station B.04.01 (Agilent, Santa Clara, California, USA). For HPLC peaks containing two or more SDS-PAGE bands, their percentual distribution was assigned by densitometry, using the Image Lab v.2.0 software (Bio-Rad, Hercules, California, USA). When SDS-PAGE bands contained more than one protein class, the percentage of each protein was assigned equally to each protein class.

2.5. *In vitro* venom activities

2.5.1. Phospholipase A_2 activity

Different amounts of venoms from *M. ruatanus*, *M. alleni*, and *M. nigrocinctus* (from 312 ng to 5 µg), dissolved in 25 µL of water, were added to 200 µL of 10 mM Tris-HCl, 10 mM $CaCl_2$, 0.1 M NaCl, pH 8.0 buffer, in microplate wells. Afterward, 25 µL of the

monodisperse synthetic substrate 4-nitro-3-octanoyloxy-benzoic acid (1 mg/mL in acetonitrile) were added [13]. After incubating for 60 min at 37 °C, the absorbance at 405 nm was determined in a microplate reader (Thermo, Waltham, Massachusetts, USA). One unit of PLA_2 activity was defined as the change of 0.001 in absorbance. Blanks omitting the venoms were included, and all assays were performed in triplicates.

2.5.2. Enzyme-linked immunosorbent assay (ELISA)

The ability of SAC-ICP equine antivenom to cross-recognize whole *M. ruatanus* venom, or its RP-HPLC fractions, was assessed by ELISA. Venoms from *M. ruatanus, M. alleni*, and *M. nigrocinctus*, respectively, were dissolved in PBS (0.12 M NaCl, 0.04 M sodium phosphate buffer, pH 7.2) and adsorbed onto 96-well microplates (Nunc) using 1 µg/100 µL/well, overnight at room temperature. After decanting the excess venom samples, wells were blocked by incubation with 100 µL of PBS containing 3% bovine serum albumin (BSA) for 30 min. Plates were washed five times with PBS and 100 µL of antivenom (serially diluted from 1:500 to 1:64,000) were added and incubated for 1 h. As a negative control, mock antivenom prepared using the plasma of a normal, non-immunized horse was run in parallel under identical conditions. After five washes with PBS, venom-bound antibodies were detected by adding anti-horse IgG/alkaline phosphatase conjugate (Sigma; 1:4000 dilution in PBS with 3% BSA) for 1 h, followed by five washes with PBS, and final color development using *p*-nitrophenylphosphate (1 mg/mL in 0.1 M glycine, pH 10.4, with 1 mM $MgCl_2$ and 1 mM $ZnCl_2$). Absorbances were recorded at 405 nm in a Multiskan microplate reader (Thermo, Waltham, Massachusetts, USA). All samples were run in

triplicate wells. ELISA titers were obtained by calculating the antivenom dilution that resulted in an absorbance of 0.5. A similar ELISA procedure was used to assess the recognition of RP-HPLC fractions of *M. ruatanus* venom by the SAC-ICP antivenom. In this case, microplates were coated with 0.4 µg/100 µL/well of each fraction, and the binding of equine antibodies was performed at an antivenom dilution of 1:1000, in PBS-BSA, as described above.

2.6. *In vivo* venom activities

Animal experiments were performed following protocols approved by the Institutional Committee for the Care and Use of Laboratory Animals of the University of Costa Rica, using CD-1 mice of both sexes, bred at Instituto Clodomiro Picado.

2.6.1. Venom lethality

In order to evaluate the lethal activity of *M. ruatanus* venom, various amounts (from 1.25 to 10 µg) dissolved in 100 µL of PBS, were injected intravenously (caudal vein) in groups of four mice (body weight between 16 and 18 g). Deaths were recorded after a period of 24 hours, and the median lethal dose (LD_{50}) was calculated by Probit analysis [14]. A similar method to determine lethal activity of the most abundant RP-HPLC fractions of *M. ruatanus* venom was used. The volume of the intravenously injected solution was 100 µl, containing 10 µg of each fraction, dissolved in PBS. Fractions 7, 8, 10, 13, 17, 20, 23, 24, 25, 26, 27, and 39 were injected.

2.6.2. Myotoxic activity

To assess the myotoxic activity, groups of five mice (18-20 g) received an intramuscular injection of 5 µg of either *M. ruatanus*, *M.alleni*, or *M. nigrocinctus* venom, in a volume of 50 µL of PBS, in the right gastrocnemius muscle. A control group received 50 µL of PBS alone. Three hours later, blood samples were taken from the tail of each mouse into heparinized capillary tubes. After centrifugation, 4 µL of plasma was used to determine the creatine kinase (CK) activity using a UV-kinetic assay (Wiener Lab, Sankt Ingbert, Germany). CK activity was expressed in units/L.

2.6.3. Neutralization of lethality

The capacity of the equine SAC-ICP antivenom to neutralize the lethal activity of *M. ruatanus* venom was estimated by pre-incubation type experiments. Groups of five mice (16-18 g) were injected intravenously with 200 µL of a solution that contained 10.6 µg of venom (equivalent to 3 x LD_{50}), previously mixed and incubated for 30 min at 37 °C with different dilutions of antivenom to obtain the following venom/antivenom ratios: 50, 100, and 200 µg of venom/mL of antivenom. Control groups of mice received the same dose of the corresponding venom, incubated with PBS instead of antivenom. Deaths were recorded after 24 h.

2.7. Statistical analyses

The significance of differences between means of two groups was assessed by Student's *t*-test, or between means of three groups by ANOVA with post-hoc Tukey HSD. Differences were considered significant if $p < 0.05$.

3. Results

3.1 The venom proteome of *M. ruatanus*

Micrurus ruatanus venom was separated into 40 fractions using RP-HPLC, which subsequently were separated into 58 bands (Fig.1). Peaks 9 and 37 were not individually analyzed by SDS-PAGE since they were considered to be part of peak 10 and peak 36, respectively. All of the SDS-PAGE bands were assigned to a protein family using tandem mass spectrometry. 3FTxs were the proteins with the highest abundance in the venom (46.4%, Fig.2), followed by PLA_2s (29.8%). A significant proportion of Kunitz-type inhibitors was also observed (10.6%). Proteins that belonged to the L-amino acid oxidase (3.4%), metalloproteinase (2.7%), C-type lectin/lectin-like (2%), serine protease (1.2%), vespryn/ohanin (0.4%), 5'-nucleotidase (0.1%), glutathione peroxidase (0.3%), and phosphodiesterase (<0.1%) families were also present, in lower amounts. *Micrurus ruatanus* venom also contained 2.9% of either peptidic or non-protein material (peaks 1-6).

3.2 *In vitro* and *in vivo* activities of *M. ruatanus* venom

As expected from its venom composition, *M. ruatanus* venom had a lower PLA_2 activity *in vitro* (Fig. 3) than the PLA_2-rich *M. nigrocinctus* venom [15] and a higher activity than *M. alleni* venom, which contains a much lower amount of PLA_2s [10]. When *M. ruatanus* venom was injected intramuscularly (i.m.) in the right gastrocnemius of mice, it was able to increase significantly plasma CK, as compared to control muscles injected with the

vehicle alone (Fig 4). Histological analysis of injected muscles confirmed the *in vivo* myotoxic activity of *M. ruatanus* venom (Fig 4). *Micrurus ruatanus* venom had a very potent lethal activity, since the intravenous (i.v.) LD_{50} in mice was 3.54 µg (95% confidence limits: 2.19 - 5.70 µg) per 16-18 g mouse. Signs compatible with respiratory paralysis were observed in injected mice.

3.3 Lethality screening analysis of major venom components of *M. ruatanus*

When injected i.v. at a dose of 10 µg, Fraction 7, which contained a 3FTx, caused the death of both mice. Fractions 17, 23, and 24 contained both 3FTxs and PLA_2s and caused also the death of the two mice injected with this dose. Fraction 25 caused the death of one mouse out of two, and only a PLA_2 was detected in this fraction. In contrast, no deaths occurred after the injection of fractions 8, 10, 13, 20, 26, 27 and 39 at a dose of 10 µg. Therefore, fractions 8, 10, 13, 20, 26, and 27 contain toxins that are not potent in its lethal effect. Fraction 39 contained an L-amino acid oxidase and a gluthathione peroxidase, which probably were denatured in the RP-HPLC process.

3.4 Immunorecognition and neutralization of *M. ruatanus* venom by SAC-ICP

The SAC-ICP antivenom was evaluated for its capacity to recognize and neutralize the lethal activity of *M. ruatanus* venom. ELISA of the whole venom (Fig.5) showed that it was recognized with a similar signal to the one obtained for *M. nigrocinctus* venom. When immunorecognition of individual RP-HPLC fractions of the venom was assessed (Fig.6), a metalloproteinase was the fraction with the highest signal, while fractions 7, 8, and 10

(3FTxs) were the least recognized toxins. Fractions that contained PLA_2s, Kunitz-type inhibitors, L-amino acid oxidases, C-type lectin/lectin like, and Vespryn/Ohanin were moderately recognized by the antivenom. When tested in the murine model, the SAC-ICP antivenom was able to neutralize the lethal activity of *M. ruatanus* up to a level of 200 µg of venom/mL of antivenom (132 mg of antivenom/ 1 mg of venom).

Discussion

The most abundant protein components in *M. ruatanus* venom belong to the 3FTx family, accounting for nearly half of its proteome. The predominance of 3FTxs has also been determined in several other *Micrurus* venoms [10,16–20], particularly in species from South America, but also extending to some of the species distributed in Central America. In this regard, *M. ruatanus* can be classified as a "3FTx-rich" venom in the proposed 3FTx/PLA_2 phenotype dichotomy for *Micrurus* venoms [10,11]. This venom composition is interesting since *M. ruatanus* was considered a subspecies of *M. nigrocinctus* by some authors for a period of time [21], but it was later classified as a distinct species [1,2]. The current analysis shows that these venoms have a different distribution of toxin families, since *M. nigrocinctus* venom is a "PLA_2-predominant" venom [15], in contrast to *M. ruatanus*. Geographically, *M. ruatanus* venom is one of the northernmost "3FTx-rich" venoms described to date, since these venoms have been found predominantly in South and Central American species, while in North America only "PLA_2-rich" *Micrurus* venoms have been described [22,23].

In vivo studies in mice revealed that *M. ruatanus* venom is one of the most toxic snake venoms in Central America, in terms of its lethal activity (LD_{50}). The i.v. LD_{50} of *M. ruatanus* venom was very similar to the i.v. LD_{50} of the yellow bellied sea snake *Hydrophis platurus* [24], which was described as the Central American snake with the lowest reported LD_{50} in murine models so far. *Micrurus ruatanus* also induced significant myotoxicity in mice. In humans, muscle necrosis due to coral snakebites is not common [6]. Based on its proteomic composition, as well as signs observed in the injected mice, the expected main clinical effects of *M. ruatanus* venom in humans would be neurotoxic effects that could lead to respiratory paralysis.

The potent lethal effect of the whole venom of *M. ruatanus* is also observed in several fractions that contain 3FTxs, or both 3FTxs and PLA_2s. Notably, fractions 8, 10, 13, 20, 26, and 27 contained 3FTxs that did not display lethal activity at the dose tested. The pharmacological effects of these fractions remain to be elucidated. Some 3FTxs with no lethal activity have been reported in other Central American coral venoms, such as *M. clarki* venom [20], or in *M. dumerilii* from Colombia (unpublished data).

The anticoral antivenom produced at Instituto Clodomiro Picado using *M. nigrocinctus* venom as immunogen was able to cross-recognize the whole venom of *M. ruatanus* with a similar intensity (ELISA titer of 12687) to the one obtained for *M. nigrocinctus* venom (ELISA titer of 14161), underscoring a close immunological similarity despite the departed patterns of predominant toxins. As previously observed with other coral snake venoms

[20], the most hydrophilic 3FTxs (such as fractions 7, 8, and 10) are recognized with a lower intensity than other fractions, while more hydrophobic and/or larger toxins are recognized with a higher intensity. The lethal activity of *M. ruatanus* venom was successfully neutralized by preincubation with the SAC-ICP antivenom, up to a dose of 200 µg of venom/mL of antivenom. Therefore, it is proposed that this antivenom would be effective in the treatment of envenomings by *M. ruatanus.*

Concluding remarks

The proteomic composition and toxicological characterization of the venom of *M. ruatanus* have been studied. *Micrurus ruatanus* venom is composed mainly by 3FTxs, with a significant amount of PLA_2s also present. Smaller amounts of L-amino acid oxidase, metalloproteinase, C-type lectin/lectin-like, serine protease, vespryn/ohanin, 5'-nucleotidase, glutathione peroxidase, and phosphodiesterase proteins were also found. *M. ruatanus* possesses a potent lethal activity, as well as a significant myotoxic activity in mice. The anticoral antivenom produced by Instituto Clodomiro Picado was able to immunorecognize the whole venom and neutralize its lethal activity. Even though bites by *M. ruatanus* are rare, its high toxicity suggests that severe envenomings can occur and, therefore, the provision of antivenom to the health facilities in Roatan Island is recommended. Since this study was performed with the venom of a single individual, there is still some degree of uncertainty if the reported venom phenotype is representative of the entire species.

Figure 1; *Micrurus ruatanus* (A) and separation of its venom proteins by RP-HPLC (B), followed by SDS-PAGE (C). Venom was fractionated on a C18 column and eluted with an acetonitrile gradient (dashed line), as described in Methods. Fractions were further separated by SDS-PAGE under reducing conditions. Molecular weight markers (Mw) are indicated in kDa. Stained bands were excised, in-gel digested with trypsin, and subjected to MALDI-TOF/TOF for assignment to protein families, as shown in Table 1.

Figure 2: Composition of *Micrurus ruatanus* venom proteome according to protein families, expressed as percentages of the total protein content. 3FTx: three-finger toxin; PLA_2: phospholipase A_2; LAO: L-amino acid oxidase; CTL: C-type lectin/lectin-like; MP: metalloproteinase, SP: serine proteinase; PDE: phosphodiesterase; KUN: Kunitz-type serine proteinase inhibitor; 5'NU: 5'-nucleotidase; GPO: Glutathione peroxidase; VSP: vespryn/ohanin; UNK: unknown/unidentified.

Figure 3: Phospholipase A_2 activity of the venoms of *Micrurus ruatanus, M. alleni*, and *M. nigrocinctus* on the monodisperse synthetic substrate 4-nitro-3-octanoyloxy-benzoic acid. Varying amounts of the venoms were incubated with the substrate for 60 min at 37 °C and the absorbance changes were recorded at 405 nm. One unit is defined as a change of 0.001 in absorbance under these conditions. Each point represents mean ± SD of triplicates.

Figure 4: Assessment of myotoxic activity in the venoms of *Micrurus ruatanus* and *M. nigrocinctus.* Plasma creatine kinase (CK) activity (A) was determined 3 h after the i.m. injection of 5 µg/50 µL of the venoms in the right gastrocnemius of mice. PBS vehicle alone (50 µL) was injected in the control group. Bars represent mean ± SD of five mice. The differences between CK activity values of PBS and *M. nigrocinctus* venom, or between PBS and *M. ruatanus* venom are significant (p<0.05). Histological evaluation of muscles injected with PBS (B) or with *Micrurus ruatanus* venom (C), after 3 h, confirmed widespread muscle necrosis in the latter.

Figure 5: Assessment of the ELISA cross-recognition of *Micrurus ruatanus* and *M. alleni* crude venoms by the equine antivenom to *Micrurus nigrocinctus*. Each venom was adsorbed to microplates and incubated with various dilutions of antivenom or normal horse serum. Bound antibodies were detected by an anti-horse IgG/alkaline phosphatase conjugate, as described in Methods. Each point represents mean ± SD of triplicates.

Figure 6: Immunorecognition of the RP-HPLC fractions of *Micrurus ruatanus* venom by an equine antivenom raised against *M. nigrocinctus* venom (SAC-ICP), as evaluated by ELISA. Venom fractions (0.4 µg/well) were adsorbed onto microplates, and the binding of antibodies was detected as described in Methods, using anti-equine immunoglobulins conjugated to alkaline phosphatase, followed by color development using *p*-nitrophenylphosphate substrate. Mock antivenom prepared using the plasma of a

normal, non-immunized horse, was used as a negative control for background. Each bar represents mean ± SD of triplicate wells. Colored circles above the bars indicate the protein family identified in each chromatographic fraction: three-finger toxin (3FTx), phospholipase A_2 (PLA_2), and Kunitz-type serine protease inhibitor (Kun), Vespryn/Ohanin, C-type lectin, Metalloproteinase, L-amino acid oxidase (LAO).

Acknowledgements

Financial support was provided by Vicerrectoría de Investigación, Universidad de Costa Rica (VI-UCR-B7608). The work of Enikő Lippa and Ferenc Török at Instituto Clodomiro Picado was supported by a scholarship from Campus Mundi International Internship Program of Tempus Public Foundation, Hungary.

Conflict of interest statement

Aarón Gómez, Greivin Corrales, Danilo Chacón, Mahmood Sasa, José María Gutiérrez, Bruno Lomonte and Julián Fernández work at Instituto Clodomiro Picado, where the antivenom used in this study is produced.

References

[1] L.D. Wilson, The status of Micrurus ruatanus (Günther), a coral snake endemic to the Bay Islands of Honduras., Herpetol. Rev. 15 (1984) 67.

[2] J.A. Campbell, W.W. Lamar, The Venomous Reptiles of the Western Hemisphere, 2nd ed., Comstock Publishing Associates, Ithaca, New York, 2004.

[3] L. Marineros, J. Porras-Orellana, M. Espinal, J. Mora, L. Valdés-Orellana, Conociendo las serpientes venenosas de Honduras, Heliconia Ideas y Publicaciones, 2012.

[4] L.D. Wilson, J.R. McCranie, J.B. Slowinski, Micrurus ruatanus, Cat. Am. Amphib. Reptil. (1992) 545.

[5] F. Bucaretchi, S. Hyslop, R.J. Vieira, A.S. Toledo, P.R. Madureira, E.M. de Capitani, Bites by coral snakes (Micrurus spp.) in Campinas, State of São Paulo, Southeastern Brazil., Rev. Inst. Med. Trop. Sao Paulo. 48 (2006) 141–5. doi:/S0036-46652006000300005.

[6] F. Bucaretchi, E.M. De Capitani, R.J. Vieira, C.K. Rodrigues, M. Zannin, N.J. Da Silva, L.L. Casais-e-Silva, S. Hyslop, Coral snake bites (*Micrurus* spp.) in Brazil: a review of literature reports, Clin. Toxicol. 54 (2016) 222–234. doi:10.3109/15563650.2015.1135337.

[7] J.J. Calvete, P. Juárez, L. Sanz, Snake venomics. Strategy and applications., J. Mass Spectrom. 42 (2007) 1405–14. doi:10.1002/jms.1242.

[8] J.J. Calvete, L. Sanz, Y. Angulo, B. Lomonte, J.M. Gutiérrez, Venoms, venomics, antivenomics., FEBS Lett. 583 (2009) 1736–43. doi:10.1016/j.febslet.2009.03.029.

[9] J.J. Calvete, Snake venomics: from the inventory of toxins to biology., Toxicon. 75

(2013) 44–62. doi:10.1016/j.toxicon.2013.03.020.

[10] J. Fernández, N. Vargas-Vargas, D. Pla, M. Sasa, P. Rey-Suárez, L. Sanz, J.M. Gutiérrez, J.J. Calvete, B. Lomonte, Snake venomics of Micrurus alleni and Micrurus mosquitensis from the Caribbean region of Costa Rica reveals two divergent compositional patterns in New World elapids, Toxicon. 107 (2015) 217–233. doi:10.1016/j.toxicon.2015.08.016.

[11] B. Lomonte, P. Rey-Suárez, J. Fernández, M. Sasa, D. Pla, N. Vargas, M. Bénard-Valle, L. Sanz, C. Corrêa-Netto, V. Núñez, A. Alape-Girón, A. Alagón, J.M. Gutiérrez, J.J. Calvete, Venoms of Micrurus coral snakes: Evolutionary trends in compositional patterns emerging from proteomic analyses, Toxicon. 122 (2016) 7–25. doi:10.1016/j.toxicon.2016.09.008.

[12] B. Lomonte, J.J. Calvete, Strategies in “snake venomics” aiming at an integrative view of compositional, functional, and immunological characteristics of venoms., J. Venom. Anim. Toxins Incl. Trop. Dis. 23 (2017) 26. doi:10.1186/s40409-017-0117-8.

[13] M. Holzer, S.P. Mackessy, An aqueous endpoint assay of snake venom phospholipase A2, Toxicon. 34 (1996) 1149–1155. doi:10.1016/0041-0101(96)00057-8.

[14] D. Finney, Statistical methods in biological assay, Charles Griffin and Company, London, 1971.

[15] J. Fernández, A. Alape-Girón, Y. Angulo, L. Sanz, J.M. Gutiérrez, J.J. Calvete, B. Lomonte, Venomic and antivenomic analyses of the Central American coral snake, Micrurus nigrocinctus (Elapidae)., J. Proteome Res. 10 (2011) 1816–27.

doi:10.1021/pr101091a.

[16] P. Rey-Suárez, V. Núñez, J.M. Gutiérrez, B. Lomonte, Proteomic and biological characterization of the venom of the redtail coral snake, Micrurus mipartitus (Elapidae), from Colombia and Costa Rica, J. Proteomics. 75 (2011) 655–667. doi:10.1016/j.jprot.2011.09.003.

[17] S. Aird, N. da Silva, L. Qiu, A. Villar-Briones, V. Saddi, M. Pires de Campos Telles, M. Grau, A. Mikheyev, Coralsnake Venomics: Analyses of Venom Gland Transcriptomes and Proteomes of Six Brazilian Taxa, Toxins (Basel). 9 (2017) 187. doi:10.3390/toxins9060187.

[18] C. Corrêa-Netto, I. de L.M. Junqueira-de-Azevedo, D.A. Silva, P.L. Ho, M. Leitão-de-Araújo, M.L.M. Alves, L. Sanz, D. Foguel, R.B. Zingali, J.J. Calvete, Snake venomics and venom gland transcriptomic analysis of Brazilian coral snakes, Micrurus altirostris and M. corallinus, J. Proteomics. 74 (2011) 1795–1809. doi:10.1016/j.jprot.2011.04.003.

[19] L. Sanz, D. Pla, A. Pérez, Y. Rodríguez, A. Zavaleta, M. Salas, B. Lomonte, J. Calvete, Venomic Analysis of the Poorly Studied Desert Coral Snake, Micrurus tschudii tschudii, Supports the 3FTx/PLA2 Dichotomy across Micrurus Venoms, Toxins (Basel). 8 (2016) 178. doi:10.3390/toxins8060178.

[20] B. Lomonte, M. Sasa, P. Rey-Suárez, W. Bryan, J. Gutiérrez, Venom of the Coral Snake Micrurus clarki: Proteomic Profile, Toxicity, Immunological Cross-Neutralization, and Characterization of a Three-Finger Toxin, Toxins (Basel). 8 (2016) 138. doi:10.3390/toxins8050138.

[21] J.A. Roze, New World coral snakes (Elapidae): A taxonomic and biological summary, Mem. Inst. Butantan. 46 (1982) 305–338.

[22] I. Vergara, M. Pedraza-Escalona, D. Paniagua, R. Restano-Cassulini, F. Zamudio, C.V.F. Batista, L.D. Possani, A. Alagón, Eastern coral snake Micrurus fulvius venom toxicity in mice is mainly determined by neurotoxic phospholipases A2, J. Proteomics. 105 (2014) 295–306. doi:10.1016/j.jprot.2014.02.027.

[23] M. Bénard-Valle, A. Carbajal-Saucedo, A. de Roodt, E. López-Vera, A. Alagón, Biochemical characterization of the venom of the coral snake Micrurus tener and comparative biological activities in the mouse and a reptile model, Toxicon. 77 (2014) 6–15. doi:10.1016/j.toxicon.2013.10.005.

[24] B. Lomonte, D. Pla, M. Sasa, W.-C. Tsai, A. Solórzano, J.M. Ureña-Díaz, M.L. Fernández-Montes, D. Mora-Obando, L. Sanz, J.M. Gutiérrez, J.J. Calvete, Two color morphs of the pelagic yellow-bellied sea snake, Pelamis platura, from different locations of Costa Rica: Snake venomics, toxicity, and neutralization by antivenom, J. Proteomics. 103 (2014) 137–152. doi:10.1016/j.jprot.2014.03.034.

Table 1. Assignment of the RP-HPLC isolated fractions of *Micrurus ruatanus* venom to protein families by MALDI-TOF/TOF of selected peptide ions from in-gel trypsin-digested protein bands.

Peak	%	Mass kDa approx.	Peptide ion m/z	z	MS/MS-derived peptide sequence	Conf (%)	Sco	Protein family; related protein
1-6	2.9				Peptides or non-proteinaceous components			
7	9.8	7	1696.85	1	YSAGXBTSBTCPAGBK	99	15	Three-finger toxin ; A0A194ATD7_9SAUR
			1990.9	1	B(H^{delta})ETX(B^{da})CCTENNCNR	99	17	Three-finger toxin ; A0A194ATD7_9SAUR
8A	2.6	10	1696.81	1	YSAGXBTSBTCPAGBK	99	14	Three-finger toxin ; A0A194ATD7_9SAUR
			1990.84	1	B(H^{delta})ETX(B^{da})CCTENNCNR	99	15	Three-finger toxin ; A0A194ATD7_9SAUR
8B	3.0	7	2490.26	1	XDRGCAATCPTVBPGVNXXCCK	99	15	Alpha-neurotoxin homolog ; P58370|3NO48_MICCO
			2106.04	1	GCAATCPTVBPGVNXXCCK	99	25	Alpha-neurotoxin homolog ; P58370|3NO48_MICCO
10A	2.2	10	1687.69	1	GPYNVCCSTDXCNK	99	13	Mipartoxin-I; A0A2P1BSY2_MICMP
10B	2.2	7	1687.7	1	GPYNVCCSTDXCNK	99	20	Mipartoxin-I; A0A2P1BSY2_MICMP
		7	1655.8	1	BXGPPEYCNXPPDR	man	man	Kunitz type serine protease inhibitor; Q1RPS9.1
			1783.8	1	BXGPPEYCNXPPDRK	man	man	Kunitz type serine protease inhibitor; Q1RPS9.1
11	0.7	7	1036.39	1	WGCAASCPK	99	6	Long chain neurotoxin; U3FYQ0_MICFL
			2086.96	1	GEBVCYTXFXVGPSYPEK	99	6	Long chain neurotoxin; U3FYQ0_MICFL
		7	1627.69	1	ANFPAFYYDPASHK	99	12	Kunitz-type protease inhibitor; A0A194ARF4_9SAUR
		7	1655.8	1	BXGPPEYCNXPPDR	man	man	Kunitz type serine protease inhibitor; Q1RPS9.1
			1783.8	1	BXGPPEYCNXPPDRK	man	man	Kunitz type serine protease inhibitor; Q1RPS9.1
12	1.2	7	1655.8	1	BXGPPEYCNXPPDR	man	man	Kunitz type serine protease inhibitor; Q1RPS9.1
			1783.8	1	BXGPPEYCNXPPDRK	man	man	Kunitz type serine protease inhibitor; Q1RPS9.1
13	10.4	7	1310.54	1	AXEFGCAASCPK	99	7	Three-finger toxin; A0A0H4BLZ2_9SAUR
		7	1374.57	1	XCBEFXYGGCK	82.6	5	Kunitz-type serine protease inhibitor; B2KTG1.1

		7	1655.8	1	BXGPPEYCNXPPDR	man	man	Kunitz type serine protease inhibitor; Q1RPS9.1
			1783.8	1	BXGPPEYCNXPPDRK	man	man	Kunitz type serine protease inhibitor; Q1RPS9.1
14	2.3	7	2063.12	1	GENXCFTXFSFBFHPAR	94.1	10	three-finger toxin precursor, B2BRQ6.1
		7	1655.8	1	BXGPPEYCNXPPDR	man	man	Kunitz type serine protease inhibitor; Q1RPS9.1
			1783.8	1	BXGPPEYCNXPPDRK	man	man	Kunitz type serine protease inhibitor; Q1RPS9.1
15A	1.5	14	1373.6	1	CBDFVCNCDR	99	15	Phospholipase A2; U3FYP8_MICFL
			1387.62	1	CBEFVCNCDR	99	12	Phospholipase A2; A0A2H6N4A4_MICLE
15B	1.6	7	2246.18	1	FVTCPDGENHCYTNVXGXR	97	10	three-finger toxin; P34073.1
		7	1655.8	1	BXGPPEYCNXPPDR	man	man	Kunitz type serine protease inhibitor; Q1RPS9.1
			1783.8	1	BXGPPEYCNXPPDRK	man	man	Kunitz type serine protease inhibitor; Q1RPS9.1
16A	1.6	14	1373.53	1	CBDFVCNCDR	99	16	Phospholipase A2; U3FYP8_MICFL
		14	1387.55	1	CBEFVCNCDR	99	13	Phospholipase A2; A0A2H6N4A4_MICLE
16B	0.5	7	1655.8	1	BXGPPEYCNXPPDR	man	man	Kunitz type serine protease inhibitor; Q1RPS9.1
			1783.8	1	BXGPPEYCNXPPDRK	man	man	Kunitz type serine protease inhibitor; Q1RPS9.1
17A	4.7	14	1095.54	1	APYNNBNFK	99	10	Phospholipase A2; U3FYP8_MICFL
			1373.53	1	CBDFVCNCDR	99	15	Phospholipase A2; U3FYP8_MICFL
		14	1387.54	1	CBEFVCNCDR	98.9	11	Phospholipase A2; A0A2H6N4A4_MICLE
17B	1.9	7	2673.16	1	DGFNFVTCPEGETYCYTTAXTAR	99	16	Three-finger toxin; U3FYQ5_MICFL
		7	1566.67	1	GCXSSCSWYYX(K^{ca})	99	16	3FTx; C6JUP5_MICCO
		7	1783.8	1	BXGPPEYCNXPPDRK	man	man	Kunitz type serine protease inhibitor; Q1RPS9.1
18	0.8	14	1373.5	1	CBDFVCNCDR	99	14	Phospholipase A2; U3FYN8_MICFL
			1387.52	1	CBEFVCNCDR	99	13	Phospholipase A2; A0A2H6NAU5_MICLE
		14	1714.86	1	VCYTXFXVGPSYPAK	99	12	three-finger toxin; A0A2D4P2Z1_MICSU
19A	0.7	10	1715.07	1	VCYTXFXVGPSYPAK	99	11	three-finger toxin; A0A2D4P2Z1_MICSU
19B	0.9	7	997.414	1	FGCAASCPK	99	10	Three-finger toxin; A0A0H4BLZ2_9SAUR
20A	2.5	14	1339.51	1	CBDXVCNCDR	99	7	Phospholipase; U3EPF6_MICFL
			1378.63	1	CFPSXTXYSYK	99	9	Phospholipase; U3FYP8_MICFL

20B	4.7	7	997.4	1	FGCAASCPK	man	man	Three-finger toxin; A0A0H4BLZ2_9SAUR
21	1.5	14	1339.51	1	CBDXVCNCDR	99	12	Phospholipase; U3EPF6_MICFL
22	1.2	14	2796.1	1	GAXDYADYGCYCGBGGSGTPVDEXDR	99	14	PLA-2-Den-2; R4G2S8_DENDV
23A	6.5	14	2796.08	1	GAXDYADYGCYCGBGGSGTPVDEXDR	99	13	PLA-2-Den-2; R4G2S8_DENDV
23B	1.3	7	2796.09	1	GAXDYADYGCYCGBGGSGTPVDEXDR	99	7	PLA-2-Den-2; R4G2S8_DENDV
		7	1676.76	1	MTFFT(P^{ox})GFGWTBXK	99	18	Three-finger toxin; A0A194APE1_9SAUR
24A	2.6	14	1041.4	1	AFVCNCDR	99	11	Phospholipase A2; U3FYP1_MICFL
		14	2796.09	1	GAXDYADYGCYCGBGGSGTPVDEXDR	99	14	PLA-2-Den-2; R4G2S8_DENDV
24B	0.4	7	1017.45	1	CGVSGCHXK	99	10	Three-finger toxin; U3FVH6_MICFL
			1505.64	1	XTCAADEBFCYK	99	19	Three-finger toxin; U3FVH6_MICFL
		7	1789.82	1	SAVFETTETCXPGXHK	99	8	Three-finger toxin; A0A0H4BLZ7_9SAUR
25A	1.8	14	1578.56	1	APYDDNNF(M^{ox})(M^{ox})NSK	99	10	Phospholipase A2; U3EPF6_MICFL
		14	2796.08	1	GAXDYADYGCYCGBGGSGTPVDEXDR	99	14	PLA-2-Den-2; R4G2S8_DENDV
25B	1.2	7	1702.69	1	APYDDNNFMMNSBR	98.5	8	Phospholipase A2; U3EPF6_MICFL
26A	3.6	14	2556.2	1	CCQVHDDCYGEAEKIDGCDPK	99	16	Phospholipase A2; P60044
			1702.9	1	APYDDNNFMMNSKR	95.8	6	Phospholipase A2; C0HKB8
		14	1889.19	1	WHMGHPGVAGCAVTCPR	99	11	Three-finger toxin; A0A194ASF5_9SAUR
26B	1.9	7	1789.89	1	SAVFETTETCLPGXHK	99	17	Three-finger toxin; A0A0H4BLZ7_9SAUR
			1874.9	1	WHXGHPGVAGCAVTCPR	99	17	Three-finger toxin; A0A0H4BLZ7_9SAUR
27A	0.4	50	1789.82	1	SAVFETTETCXPGXHK	99	14	Three-finger toxin; A0A0H4BLZ7_9SAUR
			1874.82	1	WHXGHPGVAGCAVTCPR	99	12	Three-finger toxin; A0A0H4BLZ7_9SAUR
27B	1.0	14	1874.77	1	WHXGHPGVAGCAVTCPR	99	8	Three-finger toxin; A0A0H4BLZ7_9SAUR
			1789.77	1	SAVFETTETCXPGXHK	98.2	8	Three-finger toxin; A0A0H4BLZ7_9SAUR
			1578.51	1	APYDDNNF(M^{ox})(M^{ox})NSK	99	10	Phospholipase A2; U3EPF6_MICFL
			1373.45	1	CBDFVCNCDR	99	12	Phospholipase A2; U3EPF6_MICFL
27C	2.4	7	1781.77	1	SAVFETTETCXPGXHK	99	11	Three-finger toxin; A0A0H4BLZ7_9SAUR

			1874.8	1	WHXGHPGVAGCAVTCPR	99	11	Three-finger toxin; A0A0H4BLZ7_9SAUR
28A	1.1	14	1373.47	1	CBDFVCNCDR	99	14	Phospholipase A2; U3FYP8_MICFL
			1387.48	1	CBEFVCNCDR	99	12	Phospholipase A2; A0A2H6N4A4_MICLE
			962.391	1	APYNBBNK	95.6	8	PLA2(IB)-Tri1; A7X418_TRIBI
28B	0.3	7	1789.78	1	SAVFETTETCXPGXHK	99	16	Three-finger toxin; A0A0H4BLZ7_9SAUR
			1874.79	1	WHXGHPGVAGCAVTCPR	99	18	Three-finger toxin; A0A0H4BLZ7_9SAUR
29A	0.3	14	1373.47	1	CBDFVCNCDR	99	15	Phospholipase A2; A0A194AT61_9SAUR
29B	0.1	7	1822.76	1	TPBXCPBG(B^{da})DVCYBK	99	8	Three-finger toxin; U3EPK7_MICFL
			1478.67	1	RXCDDSSXPFXR	99	14	Three-finger toxin; U3EPK7_MICFL
30	1.0	7	1694.67	1	TPBXCPBG(B^{da})DVCYK	99	11	Three-finger toxin; U3EPK7_MICFL
			1822.76	1	TPBXCPBG(B^{da})DVCYBK	99	17	Three-finger toxin; U3EPK7_MICFL
			1322.59	1	XCDDSSXPFXR	99	12	Three-finger toxin; U3EPK7_MICFL
			1478.68	1	RXCDDSSXPFXR	99	15	Three-finger toxin; U3EPK7_MICFL
31	1.2	7	1822.76	1	TPBXCPBG(B^{da})DVCYBK	99	7	Three-finger toxin; U3EPK7_MICFL
			1478.69	1	RVCDDSSXPFXR	99	12	Three-finger toxin; U3EPK7_MICFL
32A	0.3	15	1078.53	1	SGBHFFEVK	99	8	Vespryn; A0A194AR88_9SAUR
			936.48	1	SPPGBWHK	99	11	Vespryn; A0A194AR88_9SAUR
			1480.69	1	YGTBTEWAVGXAGK	99	14	Vespryn; A0A194AR88_9SAUR
			1510.74	1	RBGYXTYVPEER	99	15	Vespryn; A0A194AR88_9SAUR
			1226.56	1	GYXTYVPEER	99	12	Vespryn; A0A194AR88_9SAUR
			1354.65	1	BGYXTYVPEER	99	17	Vespryn; A0A194AR88_9SAUR
			2198	1	ADVTFDSNTAFGSXVVSPDBK	99	27	Vespryn; A0A194AR88_9SAUR
			1810.82	1	TVENVGVPBAVSDNPER	99	22	Vespryn; A0A194AR88_9SAUR
32B	0.2	7	1322.59	1	XCDDSSXPFXR	99	8	Three-finger toxin; U3EPK7_MICFL
			1478.68	1	RXCDDSSXPFXR	99	14	Three-finger toxin; U3EPK7_MICFL
			1694.66	1	TPBXCPBG(B^{da})DVCYK	99	14	Three-finger toxin; U3EPK7_MICFL
			1822.76	1	TPBXCPBG(B^{da})DVCYBK	99	16	Three-finger toxin; U3EPK7_MICFL
			1354.65	1	BGYXTYVPEER	99	8	Vespryn; A0A194AR88_9SAUR
			1810.81	1	TVENVGVPBAVSDNPER	99	13	Vespryn; A0A194AR88_9SAUR
			2198	1	ADVTFDSNTAFGSXVVSPDBK	99	9	Vespryn; A0A194AR88_9SAUR
33A	0.3	15	1915.78	1	WNDTPCESXFAFXCR	99	13	C-type lectin; A0A194AR98_9SAUR
			1681.77	1	EYCVHXXASEGYXK	99	17	C-type lectin; A0A194AR98_9SAUR

			1310.59	1	YTCPXDWXSR	99	12	C-type lectin; A0A194AR98_9SAUR
			1183.59	1	NVWXGXNDPR	99	15	C-type lectin; A0A194AR98_9SAUR
33B	0.5	10	1211.69	1	GXPFXPWXXR	99	14	C-type lectin; A0A194AR98_9SAUR
			1268.72	1	(G^{cm})XPFXPWXXR	98	10	C-type lectin; A0A194AR98_9SAUR
34A	1.0	15	1310.6	1	YTCPXDWXSR	99	11	C-type lectin; U3EPK2_MICFL
			1005.47	1	XWEWTDR	96.2	9	C-type lectin; U3EPK2_MICFL
34B	0.4	7	1211.69	1	GXPFXPWXXR	98.4	8	Three-finger toxin; A0A194ARB6_9SAUR
35	0.7	15	1681.77	1	EYCVHXXASEGYXK	99	19	C-type lectin; A0A194AR98_9SAUR
			2214.85	1	SSTNYTSWNEGEPNNSWNK	99	9	C-type lectin; A0A194AR98_9SAUR
			1915.78	1	WNDTPCESXFAFXCR	99	10	C-type lectin; A0A194AR98_9SAUR
			1183.59	1	NVWXGXNDPR	99	13	C-type lectin; A0A194AR98_9SAUR
			1005.46	1	XWEWTDR	95.6	10	C-type lectin; A0A194AR98_9SAUR
36A	1.9	50	2114	1	XDFNGNTXGXAHXGSXCSPK	99	14	Metalloproteinase (Type III); U3EPC7_MICFL
			1184.5	1	DMCFTXNQR	99	11	Metalloproteinase (Type III); U3EPC7_MICFL
36B	0.5	40	1544.77	1	BYXEFYVVVDNR	99	9	Metalloproteinase type III; A0A194AS47_9SAUR
			1297.53	1	SAECPTDSFBR	99	10	Metalloproteinase type III; A0A194AS47_9SAUR
			1605.82	1	SNVAVTXDXFGBWR	99	8	Metalloproteinase type III; A0A194AS47_9SAUR
			2052.9	1	TBPAYBFSSCSVBEHBR	99	8	Metalloproteinase type III; A0A194AS47_9SAUR
			1166.6	1	TSVAVVBDYGK	99	11	Metalloproteinase type III; A0A194AS47_9SAUR
			1416.68	1	YXEFYVVVDNR	99	10	Metalloproteinase type III; A0A194AS47_9SAUR
			2114	1	XDFNGNTXGXAHXGSXCSPK	99	13	Metalloproteinase type III; A0A194AS47_9SAUR
36C	0.1	25	1094.53	1	YNSNXNTXR	99	10	MP_IIa SVMP (Fragment); E3UJM0_BOTNU
			1764.86	1	SM(N^{da})VDASXANXEVWSK	99	11	MP_IIa SVMP (Fragment); E3UJM0_BOTNU
			1675.84	1	YXEXAVVADHGMF(T^{dh})K	99	16	MP_IIa SVMP (Fragment); E3UJM0_BOTNU
38A	<0.1	120	970.499	1	XHFANNVR	99	6	phosphodiesterase; A0A2D4P571_MICSU
			1504.7	1	SMEAXFXAHGPGFK	99	11	phosphodiesterase; A0A2D4P571_MICSU
			1355.62	1	AATYFWPGSEVK	99	9	phosphodiesterase; A0A2D4P571_MICSU
			2105.92	1	RPDFSTXYXEEPDTTGHK	99	14	phosphodiesterase; A0A2D4P571_MICSU
			2305.04	1	ABRPDFSTXYXEEPDTTGHK	98.8	6	phosphodiesterase; A0A2D4P571_MICSU

38B	0.1	70	1306.66	1	BVPVVBAYAFGK	99	17	Ecto-5'-nucleotidase; U3FYP9_MICFL
			1449.67	1	VVSXNVXCTECR	99	11	Ecto-5'-nucleotidase; U3FYP9_MICFL
			1389.71	1	XTXXHTNDVHAR	99	17	Ecto-5'-nucleotidase; U3FYP9_MICFL
			2406.97	1	HPDDNEWNHVSMCXVNGGGXR	99	13	Ecto-5'-nucleotidase; U3FYP9_MICFL
			1930.91	1	VXXPSFXAAGGDGYY(M^{ox})XK	99	8	Ecto-5'-nucleotidase; U3FYP9_MICFL
			1110.51	1	BAFEHSVHR	99	13	Ecto-5'-nucleotidase; U3FYP9_MICFL
			1255.71	1	FPXXSANXRPK	99	16	Ecto-5'-nucleotidase; U3FYP9_MICFL
			2689.21	1	ETPVXSNPGPYXEFRDEVEEXBK	99	19	Ecto-5'-nucleotidase; U3FYP9_MICFL
			2421.02	1	FHECNXGNXXCDAVVYNNXR	95.3	12	Ecto-5'-nucleotidase; U3FYP9_MICFL
38C	0.2	65	1388.6	1	BFWEDDGXHGGK	99	17	Amine oxidase (Fragment); A0A2H4N3D4_BOTMO
			1352.61	1	SAGBXYEESXBK	99	16	Amine oxidase (Fragment); A0A2H4N3D4_BOTMO
			1396.66	1	AGHBVTVXEASER	99	22	Amine oxidase (Fragment); A0A2H4N3D4_BOTMO
			2271	1	XYFAGEYTABAHGWXDSTXK	99	28	Amine oxidase (Fragment); A0A2H4N3D4_BOTMO
38D	0.3	30	1563.74	1	FPCAXVXEPGVYAK	99	18	Serine proteinase; A0A194AT39_9SAUR
			1944.86	1	XGVHNVHVHYEDEBXR	99	23	Serine proteinase; A0A194AT39_9SAUR
			2170.94	1	GDSGGPXXCNGBXBGXVSWGR	99	23	Serine proteinase; A0A194AT39_9SAUR
38E	0.1	25	1675.81	1	YXEXAVVADHGMF(T^{dh})K	99	18	MP_I2 SVMP (Fragment); E3UJL4_BOTNU
			1096.5	1	TXTSFGEWR	99	13	MP_I2 SVMP (Fragment); E3UJL4_BOTNU
			1096.5	1	TXTSFGEWR	99	13	BATXSVMPII1; A0A1L8D600_BOTAT
			2603.99	1	EVXSYEFSDCSBNBYETYXTK	99	9	BATXSVMPII1; A0A1L8D600_BOTAT
39A	0.2	150	1733.85	1	BDPGXFEYPVBPSEK	99	14	Amine oxidase; U3FYQ2_MICFL
			2274.98	1	XHFAGEYTANDHGWXDSTXK	99	10	Amine oxidase; U3FYQ2_MICFL
			1300.67	1	XHFBPPXPSHK	99	14	Amine oxidase; U3FYQ2_MICFL
			1833.76	1	EFVBEDENAWYYXK	99	8	Amine oxidase; U3FYQ2_MICFL
			1484.64	1	EADYEEFXEXAR	99	18	Amine oxidase; U3FYQ2_MICFL
39B	3.0	70	1733.85	1	BDPGXFEYPVBPSEK	99	15	Amine oxidase; U3FYQ2_MICFL
			1833.76	1	EFVBEDENAWYYXK	99	13	Amine oxidase; U3FYQ2_MICFL
			2274.99	1	XHFAGEYTANDHGWXDSTXK	99	28	Amine oxidase; U3FYQ2_MICFL
			1484.64	1	EADYEEFXEXAR	99	19	Amine oxidase; U3FYQ2_MICFL
			1456.77	1	RXHFBPPXPSHK	98.9	10	Amine oxidase; U3FYQ2_MICFL
			1310.6	1	RFDEXVGGFDR	99	15	Amine oxidase; A0A194ASA8_9SAUR

39C	0.3	23	1854.9	1	GDVNGENEBBXYTFXK	99	8	Glutathione peroxidase (Fragment); V8P395_OPHHA
			1329.69	1	XHDXBWNFEK	99	15	Glutathione peroxidase (Fragment); V8P395_OPHHA
40	0.9	30	1089.65	1	XBVPVBYSR	99	8	serine protease; A0A2D4PRX2_MICSU

Cysteine residues are carbamidomethylated. X: Leu/Ile; B: Lys/Gln; Confidence (Conf) and Score (Sco) values calculated by the Paragon® algorithm of ProteinPilot®. Mass kDa approx: estimated mass in SDS-PAGE in reducing conditions. Possible, although unconfirmed or ambiguous amino acid modifications suggested by the automated identification software are shown in parentheses, with the following abbreviations: ^{da}: deamidated, ^{delta}: Delta(H(2)C(2)(H), ^{ca}: carbamyl, ^{ox}:oxidation, ^{cm}: carbamidomethyl, ^{dh}: dehydrated.

Highlights

- The proteomic characterization of *Micrurus ruatanus* venom has been determined.
- Toxicity, immunorecognition, and neutralization of the venom were also determined.
- The venom displayed a three-finger toxin-rich phenotype.
- Venom lethal activity in mice was neutralized by an anticoral antivenom.
- Major fractions with lethal activity were also identified.

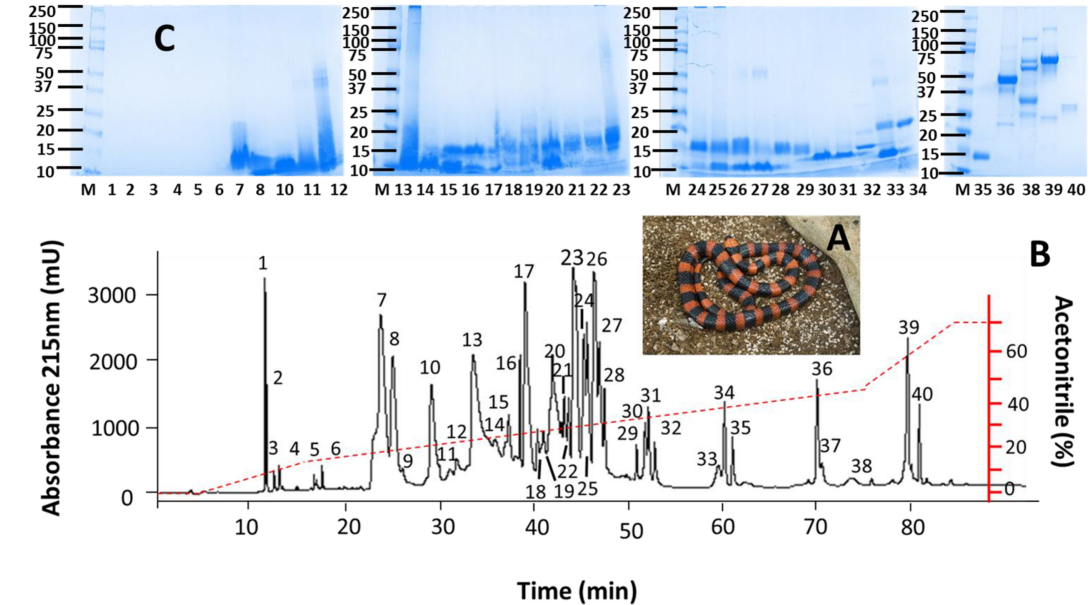
C
250
150
100
75
50
37
25
20
15
10
M 1 2 3 4 5 6 7 8 10 11 12
M 13 14 15 16 17 18 19 20 21 22 23
M 24 25 26 27 28 29 30 31 32 33 34
M 35 36 38 39 40
A
B
Absorbance 215nm (mU)
3000
2000
1000
0
Acetonitrile (%)
60
40
20
0
10
20
30
40
50
60
70
80
Time (min)

Figure 1

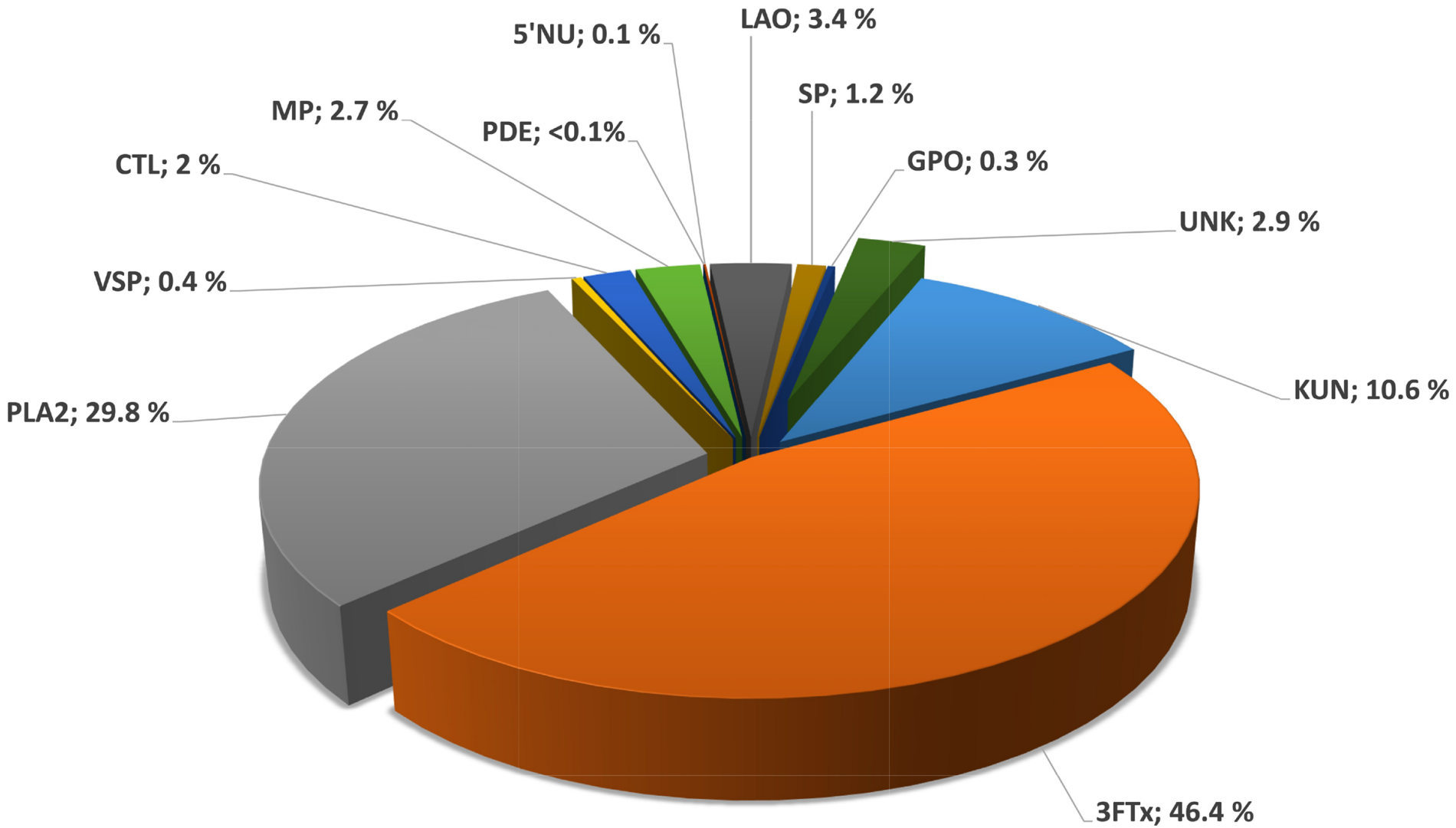
5'NU; 0.1 %
LAO; 3.4 %
SP; 1.2 %
MP; 2.7 %
PDE; <0.1%
GPO; 0.3 %
CTL; 2 %
UNK; 2.9 %
VSP; 0.4 %
KUN; 10.6 %
PLA2; 29.8 %
3FTx; 46.4 %

Figure 2

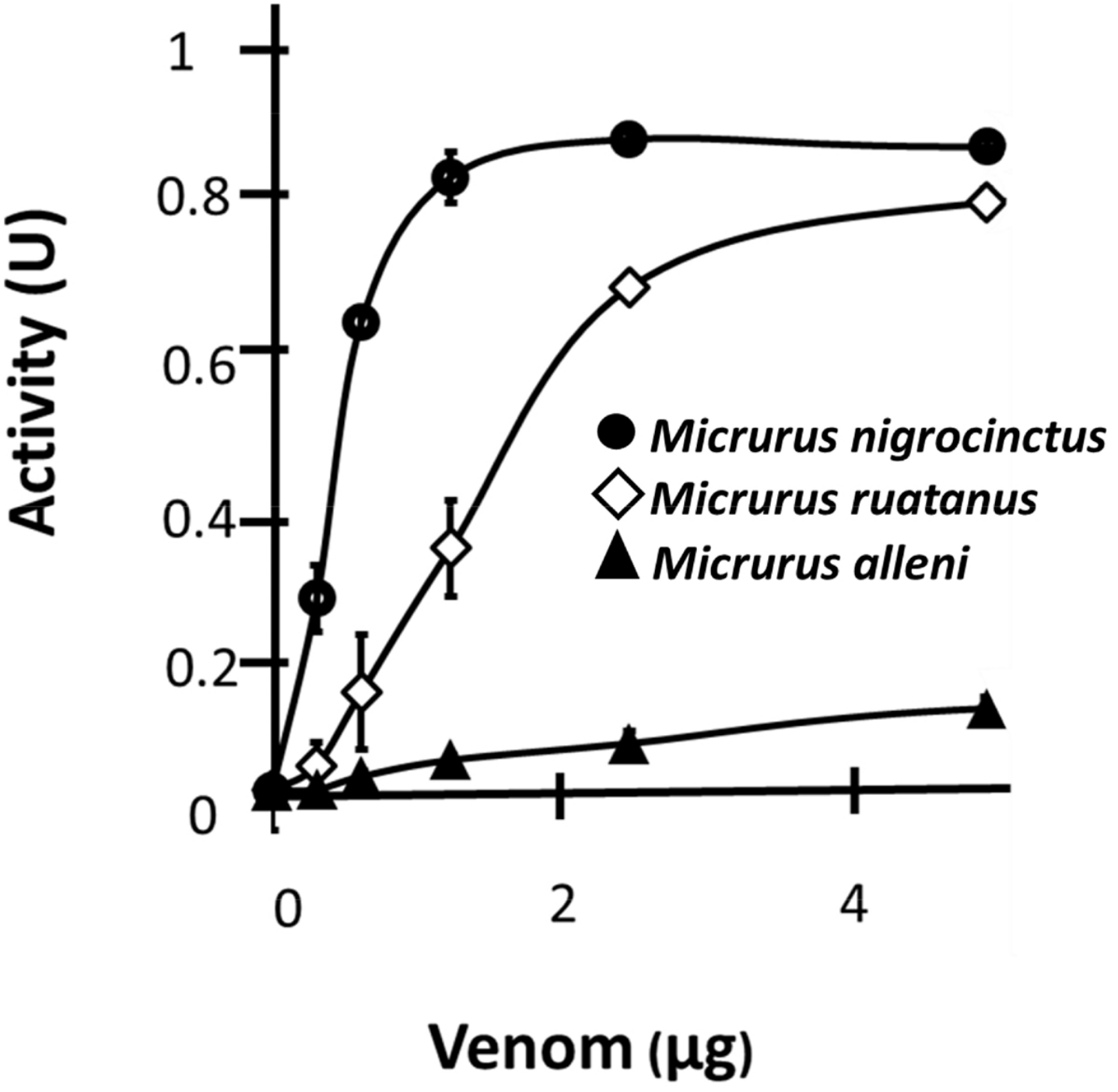
Activity (U)
1
0.8
0.6
0.4
0.2
0
0
2
4
Venom (µg)
Micrurus nigrocinctus
Micrurus ruatanus
Micrurus alleni

Figure 3

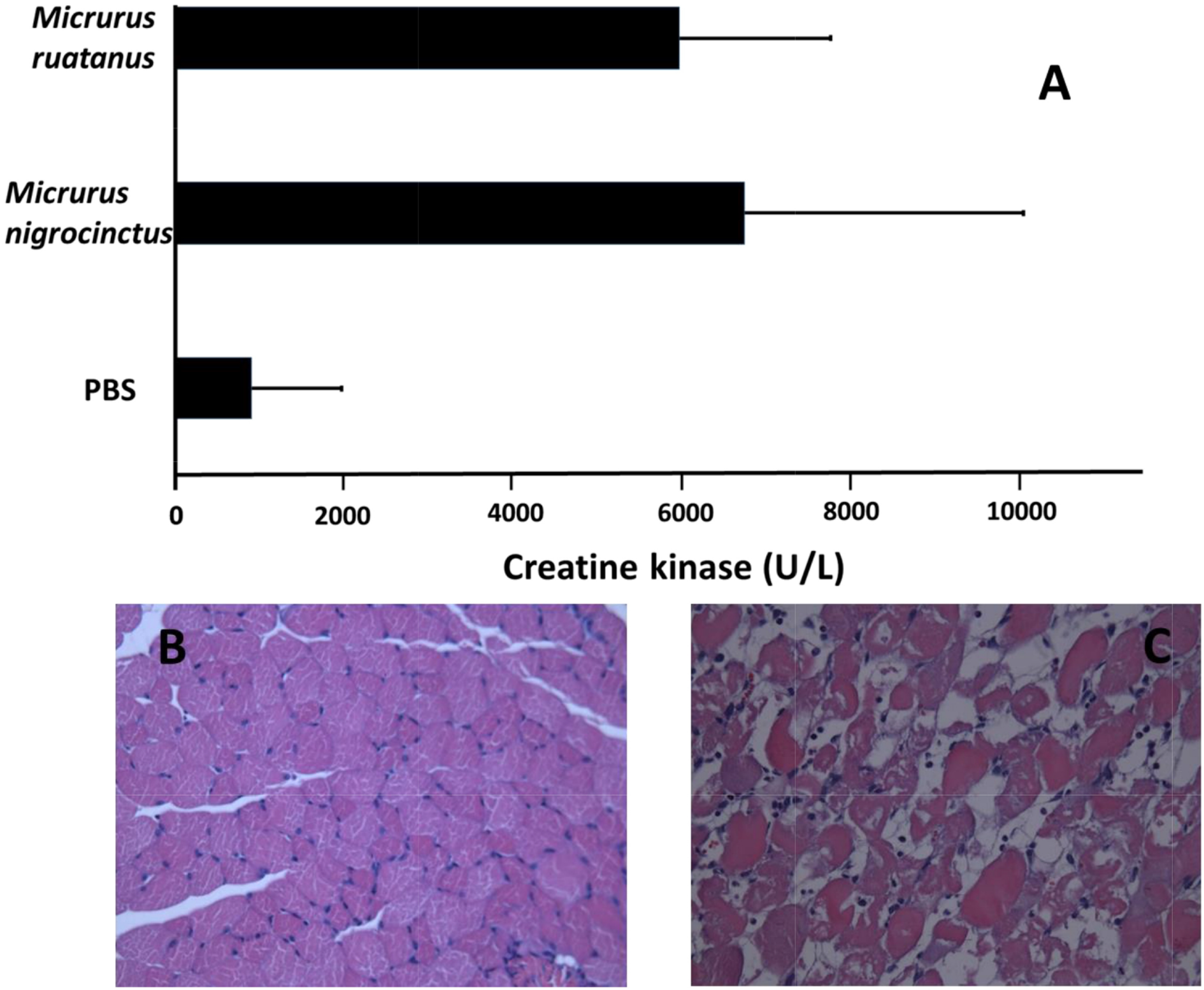
Micrurus ruatanus
Micrurus nigrocinctus
PBS
A
0
2000
4000
6000
8000
10000
Creatine kinase (U/L)
B
C

Figure 4

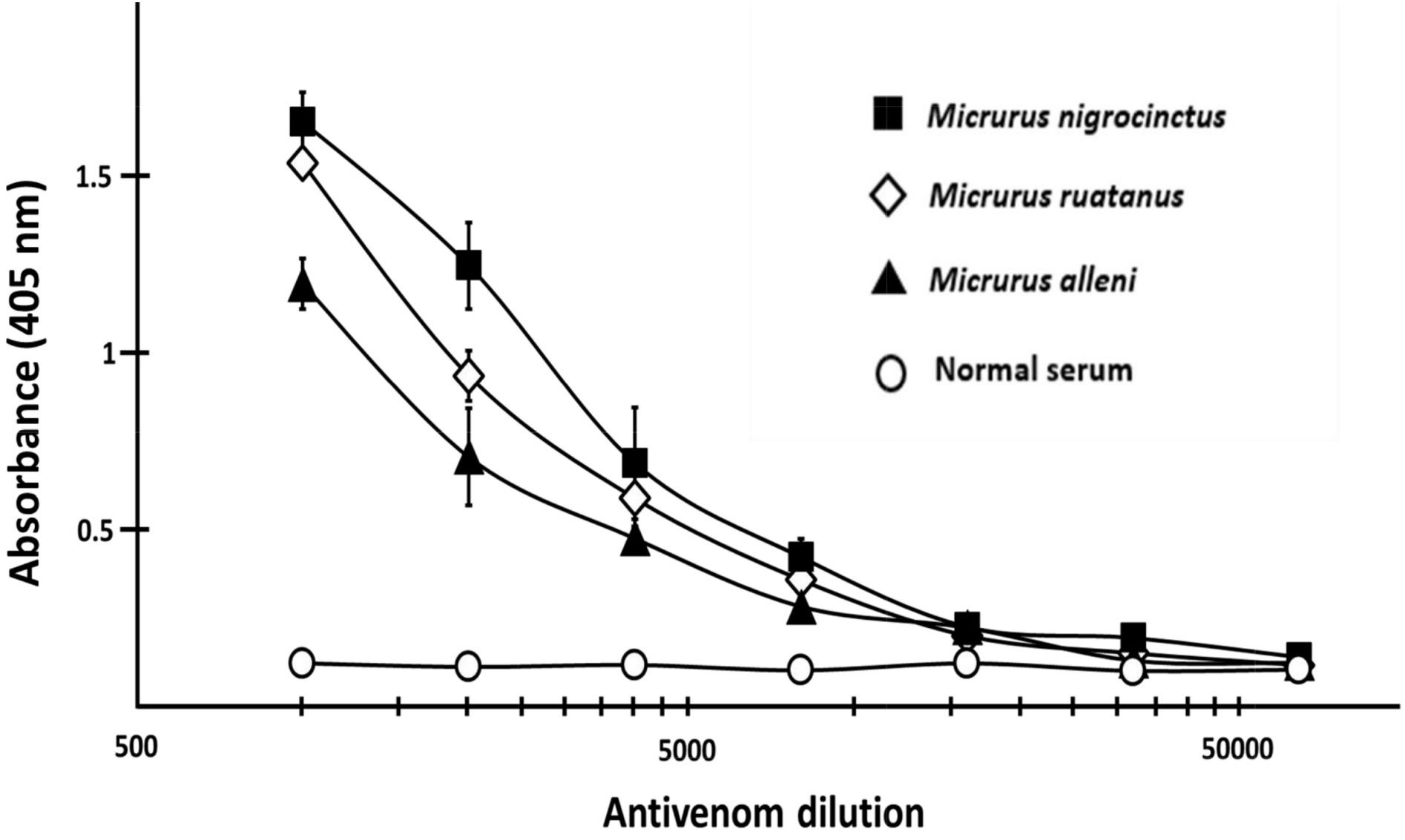
Micrurus nigrocinctus
Micrurus ruatanus
Micrurus alleni
Normal serum
Absorbance (405 nm)
1.5
1
0.5
500
5000
50000
Antivenom dilution

Figure 5

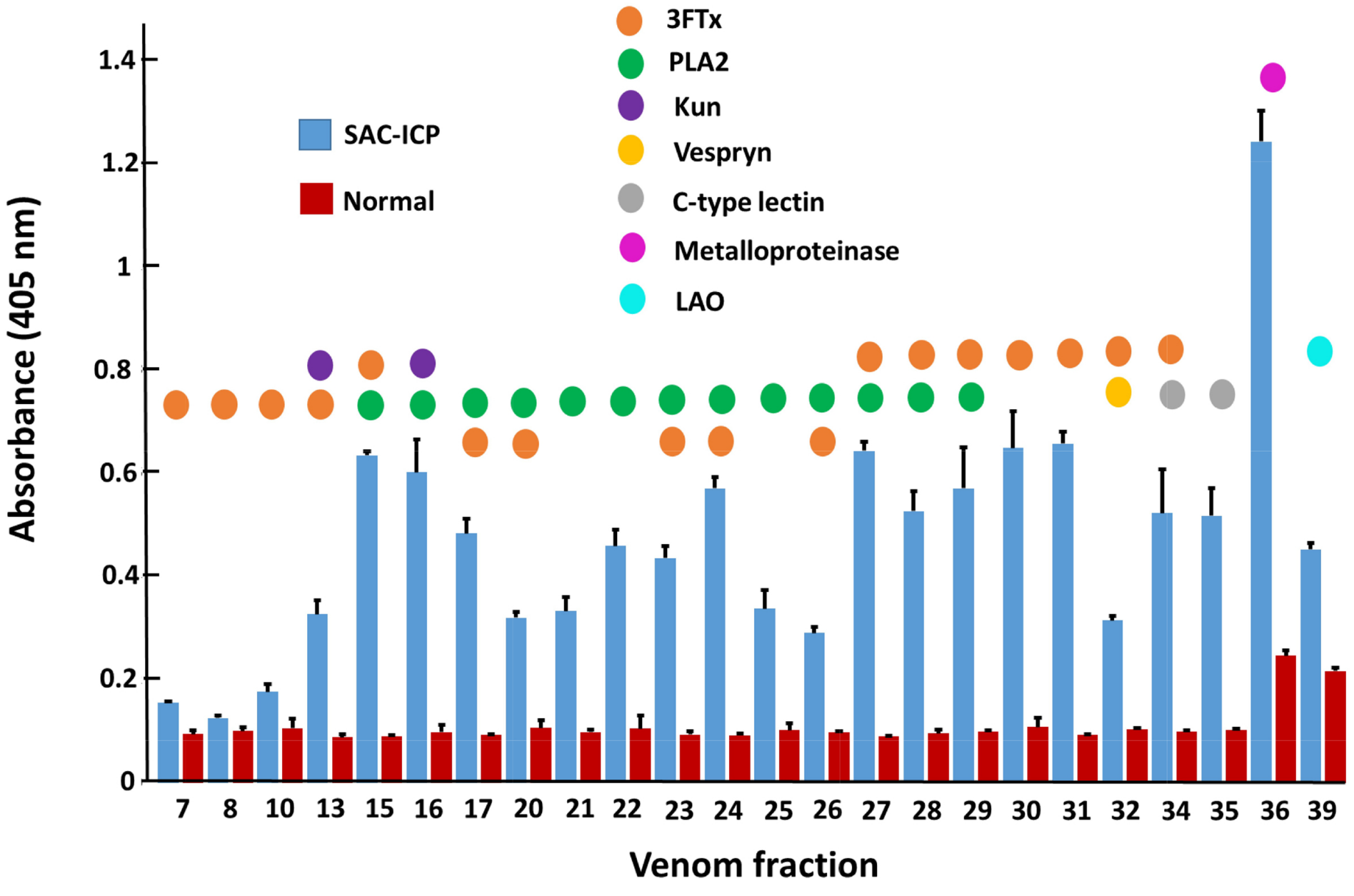
3FTx
PLA2
Kun
Vespryn
C-type lectin
Metalloproteinase
LAO
SAC-ICP
Normal
Absorbance (405 nm)
1.4
1.2
1
0.8
0.6
0.4
0.2
0
7 8 10 13 15 16 17 20 21 22 23 24 25 26 27 28 29 30 31 32 34 35 36 39
Venom fraction

Figure 6